The Effect of Chemical and Nanotopographical Modifications on the Early Stages of Osseointegration

Luiz Meirelles, DDS, PhD[1]/Fredrik Currie, PhD[2]/Magnus Jacobsson, MD, PhD[3]/
Tomas Albrektsson, MD, PhD[4]/Ann Wennerberg, DDS, PhD[5]

Purpose: To investigate the effect of chemically modified implants with similar microtopographies but different nanotopographies on early stages of osseointegration. **Materials and Methods:** Forty screw-shaped implants were placed in 10 New Zealand white rabbits. The implant surface modifications investigated in the present study were (1) blasting with TiO_2 and further (2) fluoride treatment or (3) modification with nano-hydroxyapatite. Surface evaluation included topographical analyses with interferometry, morphologic analyses with scanning electron microscopy, and chemical analyses with x-ray photoelectron spectroscopy. Bone response was investigated with the removal torque test, and histologic analyses were carried out after a healing period of 4 weeks. **Results:** Surface roughness parameters showed a slight decrease of the average height deviation for the fluoride-treated compared to the blasted (control) and nano-hydroxyapatite implants. Scanning electron microscopic images at high magnification indicated the presence of nanostructures on the chemically modified implants. Chemical analyses revealed the presence of titanium, oxygen, carbon, and nitrogen in all implant groups. The blasted-fluoride group revealed fluoride, and the blasted-nano HA group calcium and phosphorus with simultaneous decrease of titanium and oxygen. Removal torque values revealed an increased retention for the chemically modified implants that exhibit specific nanotopography. The histologic analyses demonstrated immature bone formation in contact with the implant surface in all groups, according to the healing period of the experiment. **Conclusion:** Chemical modifications used in the present study were capable of producing a particular nanotopography, and together with the ions present at the implant surface, may explain the increased removal torque values after a healing period of 4 weeks. INT J ORAL MAXILLOFAC IMPLANTS 2008;23:641–647

Key words: dental implants, hydroxyapatite, nanotopography, osseointegration, surface modification, titanium fluoride

[1]Postdoctoral Researcher, Sahlgrenska Academy at Göteborg University, Institute of Odontology, Department of Prosthodontics/Dental Materials Science, Göteborg, Sweden.
[2]Production Manager, Promimic, Göteborg, Sweden.
[3]Medical Director and Vice President for Research and Development, Astra Tech, Mölndal, Sweden.
[4]Professor and Head, Sahlgrenska Academy at Göteborg University, Institute of Clinical Sciences, Department of Biomaterials, Göteborg, Sweden.
[5]Professor and Head, Department of Prosthetic Dentistry, Faculty of Odontology, Malmö University, Malmö, Sweden.

Correspondence to: Dr Luiz Meirelles, Sahlgrenska Academy at Göteborg University, Institute of Odontology, Department of Prosthetic Dentistry, Göteborg, Sweden. E-mail: luiz.meirelles@odontologi.gu.se

Early events that take place after oral implant insertion are in part dictated by biomolecules that interact with the material surface.[1] Several components of the initial healing cascade are on the nanometer scale, and the binding sites where they interact are even smaller.[2,3] Furthermore, the lamellar bone formed at the interface after an adequate healing phase exhibits nanostructures, such as abundant collagen fibrils and apatite crystals.[4] Currently, most commercially available oral implants are moderately rough on the micrometer scale[5]; however, no specific attention has been given to investigating an implant surface with nanostructures. The in vitro influence of nanostructures on cell activity has been demonstrated with different cell types,[6] which indicates that surface nanotopography may modulate the final tissue formation.

Despite high success rates obtained with the correct protocol, in some specific cases the results of titanium implant rehabilitation are unfavorable.[7–9] The factors underlying implant success or failure
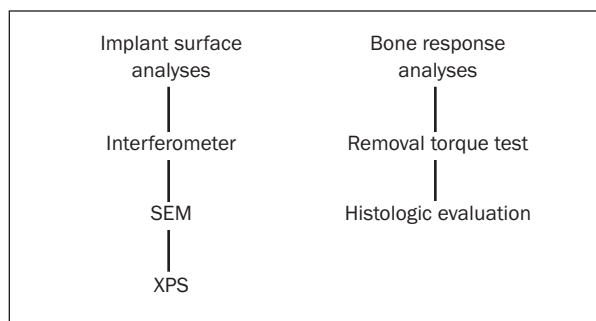
Fig 1 Diagrams of the evaluation techniques used for implant surface and bone response analyses. Interferometer examination provides quantitative and qualitative analyses of the surface microtopography. Scanning electron microscopy (SEM) images reveal the surface morphology of structures up to the nanoscale. The chemical composition of the implant surface was monitored by x-ray photoelectron spectroscopy (XPS). Quantitative and qualitative bone response analyses were performed with the removal torque test and histologic evaluation, respectively.

have been investigated in numerous scientific reports. However, the mechanisms that explain the reasons for success or failure are not fully understood. Nanotechnology has emerged and proven to be a successful path to add knowledge to the field for both production and characterization of nano-sized structures at the implant-tissue interface. Thus, the implementation of specific nanostructures at the implant surface may represent an alternative to improve the overall success rate of dental implants in unfavorable cases and a way to increase knowledge of the osseointegration phenomena.

The New Zealand white rabbit is a widely accepted model to investigate bone response to titanium implants.[10,11] The results of the animal experiments indicate the potential benefits of titanium implant modifications that may improve rehabilitation with bone-anchored implants. Recently, the results of an in vivo study supported the importance of nano-hydroxyapatite (nano-HA) structures that altered the early bone response in a rabbit model despite reduced micrometer roughness.[12] In the present study, nanostructures (ranging from 1 to 100 nm) were combined with microstructures (ranging from 1 to 100 μm) present in the precursor surface, and the final bone response was dependent on the synergetic effects of the surface chemistry combined with both micro- and nanoscale structures of the implants. Therefore, the aim of the present study was to evaluate the effect of nanostructures created by fluoride treatment[13] and nano-HA modification[14] on bone formation after 4 weeks of healing.

MATERIALS AND METHODS

Implant and Surface Modification

A total of 40 threaded titanium implants (Astra Tech, Mölndal, Sweden) with an external diameter of 3.5 mm and a total length of 7.5 mm were used in this study. The surface modifications included blasting with TiO_2 either (1) treated with dilute hydrofluoric acid or (2) modified with nano-HA. Thus, the blasted implants acted as the control of the experiment at the same time as the underlying topography for the tested surface modifications.

Animals and Surgery Technique

New Zealand white female rabbits were used in this study, which was approved by the local ethical committee at Göteborg University. All animals were adult (9 months old) and had a mean weight of 4.9 kg. A total of 40 implants were inserted in 10 rabbits. Implant insertion was randomized and blinded, and each rabbit received 1 implant from each group (2 implants/leg). The different implants could not be distinguished by the naked eye. The blasted fluoride-treated group was duplicated (F1 and F2) as a control of the experimental design. Thus, this experiment comprised 4 groups with 3 different surfaces, ie, (1) blasted control, (2) F1 implants, (3) F2 implants, and (4) nano-HA implants.

The animals were anesthetized with intramuscular injections of fentanyl 0.3 mg/mL and fluanisone 10 mg/mL (Hypnorm Vet, Janssen Pharmaucetica, Beerse, Belgium) at a dose of 0.5 mL/kg of body weight and intraperitoneal injections of diazepam (Stesolid Novum, Dumex Alpharma, Denmark) at a dose of 2.5 mg per animal. If necessary, anesthesia was maintained using additional doses of fentanyl and fluanisone at a dose of 0.1 ml/kg body weight. Before surgery 1 mL of lidocaine (Xylocain, Astra Zeneca, Södertälje, Sweden) was administered subcutaneously in the intended surgical sites. The experimental sites were opened via incisions through skin and fascia, and the bone surfaces exposed with the aid of an elevator. The implants were placed after preparation with guide and twist drills of 2.0 and 3.2 mm in diameter. During all surgical drilling sequences, low rotational speed with profuse saline cooling was used. The wounds were closed by suturing the fascia and skin separately. The animals were allowed to run freely after surgery.

Surface Characterization

Surface characterization and bone response evaluation methods are summarized in Fig 1. Topographical analysis was performed using an interferometer (MicroXAM, PhaseShift, Tucson, AZ) with a measure-

ment area of 260 × 200 μm. A Gaussian filter (size 50 × 50 μm) was selected to remove errors of form and waviness. Three specimens of each group were selected at random and measured on 3 thread tops, thread valleys, and flanks. The 3-dimensional roughness parameters calculated were the arithmetic average height deviation (S_a), the density of summits (S_{ds}), and the developed surface area ratio (S_{dr}). Morphologic study of the implant surfaces was performed with scanning electron microscopy (SEM) using a LEO Ultra 55 FEG, operating between 1 and 7 kV. Chemical composition of the implant surfaces was monitored with x-ray photoelectron spectroscopy (XPS) using a PHI 5500 (Perkin Elmer, Physical Electronics Division, Waltham, MA). Monochromatic AlKα x-ray radiation operated at 350 W was utilized, and the relative energy scale was fixed with C 1s.

Evaluations of the Bone Response

The follow-up time was 4 weeks. After this period, animals were anaesthetized as described and sacrificed with an overdose of pentobarbital 60 mg/mL (Pentobarbitalnatrium, Apoteksbolaget, Sweden). Of the total of 40 implants inserted, 8 implants placed proximally in the right tibia were selected for histological analyses (2 implants per group), and the remaining 32 implants were used for the removal torque test (8 implants per group). Histologic analyses of undecalcified cut and ground sections[15] were analyzed with a light microscope (Eclipse 600, Nikon, Tokyo, Japan). Histomorphometric evaluations of bone-implant contact in all implant threads were calculated with an image software analysis program (Image Analysis 2000, Tekno Optik, Sweden). The biomechanical test of the implant-bone interface was performed with the removal torque test. The removal torque instrument is an electronic instrument (Detektor, Göteborg, Sweden) involving a strain gauge transducer used for testing the implant stability (peak loosening torque in Ncm) in the bone bed and thus can be regarded as a 3-dimensional test roughly reflecting the interfacial shear strength between bone tissue and the implant.[13,16,17] A linearly increasing torque was applied on the same axis of the implant until failure of integration was reached, and the peak value was recorded.

Statistical Analysis

Statistical analyses of removal torque values were performed with the Wilcoxon signed rank test. Differences were considered statistically significant at $P \leq .05$.

Table 1   Optical Interferometry Surface Roughness (Mean ± SD)

Implant	Sa (μm) Mean	SD	Sdr (%) Mean	SD	Sds (μm^{-2}) Mean	SD
Blasted	1.42	0.22	30.1	2.7	0.1	0.0
Blasted-F1	1.26	0.23	29.2	3.7	0.1	0.0
Blasted-F2	1.24	0.23	28.0	4.6	0.1	0.0
Blasted-nano HA	1.36	0.18	30.3	5.6	0.1	0.0

RESULTS

Surface Evaluation

Optical interferometer microscopy data showed that all implants were moderately rough. The surface roughness mean values for the blasted, F1, F2, and nano-HA implants were, respectively, 1.42 μm, 1.26 μm, 1.24 μm, and 1.36 μm in average height deviation (S_a); 30.1, 29.2, 28.0, and 30.3% of developed surface ratio (S_{dr}). The number of summits per sampling area (S_{ds}) for all surfaces investigated was 0.1 μm^{-2} (Table 1). Three-dimensional images of the optical interferometer measurements from the tip of the thread can be observed in Fig 2. The morphologic evaluation of each surface was performed with SEM (Fig 3). Implant surfaces observed at 1,500× exhibited similar microtopography for the blasted control and nano-HA implants. The fluoride-treated implants were slightly smoother, with less pronounced sharp edges and a coral-like topography. At increased magnification (20,000×), nanostructures were present on both fluoride-treated and nano-HA implants, revealing a particular nanotopography for those implants combined with the microtopography. At higher magnification (125,000×) the nanostructures produced by the fluoride treatment and by the nano-HA modification could be observed in more detail. Such small structures were not observed on the blasted control implants (Fig 3c). XPS spectra of the blasted implants revealed binding energy correspondent to oxygen, titanium, carbon, and traces of nitrogen. The fluoride-treated implants revealed the same elements plus fluoride at a relative atomic concentration of 1.0%. The nano-HA implants revealed calcium and phosphorus elements with reduced concentrations of titanium compared to the other groups. All implants had a similar concentration of carbon contaminants. XPS as well as SEM implant surface analyses showed similar results for the F1 and F2 implants and were not presented in duplicate here.
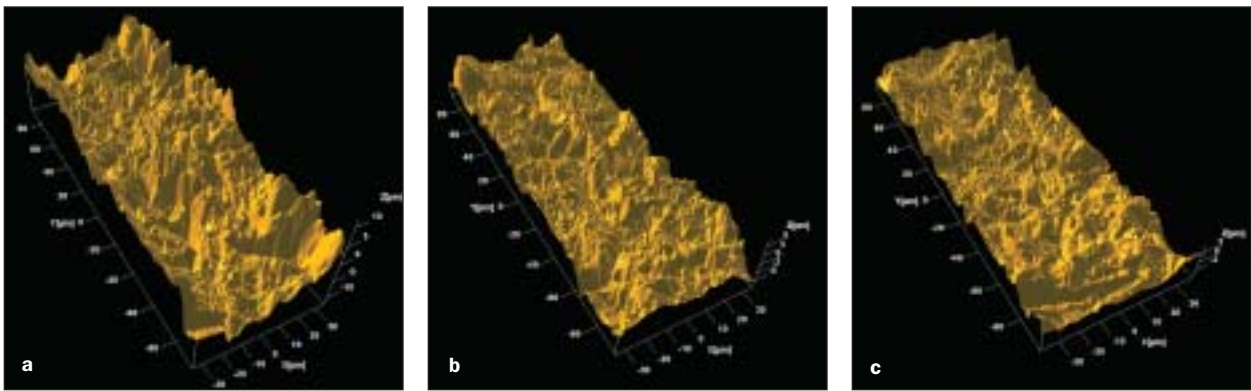
Fig 2 Optical interferometer images of measurements from the tip of the thread. *(a)* Blasted, *(b)* fluoride-treated, and *(c)* nano-HA implants.
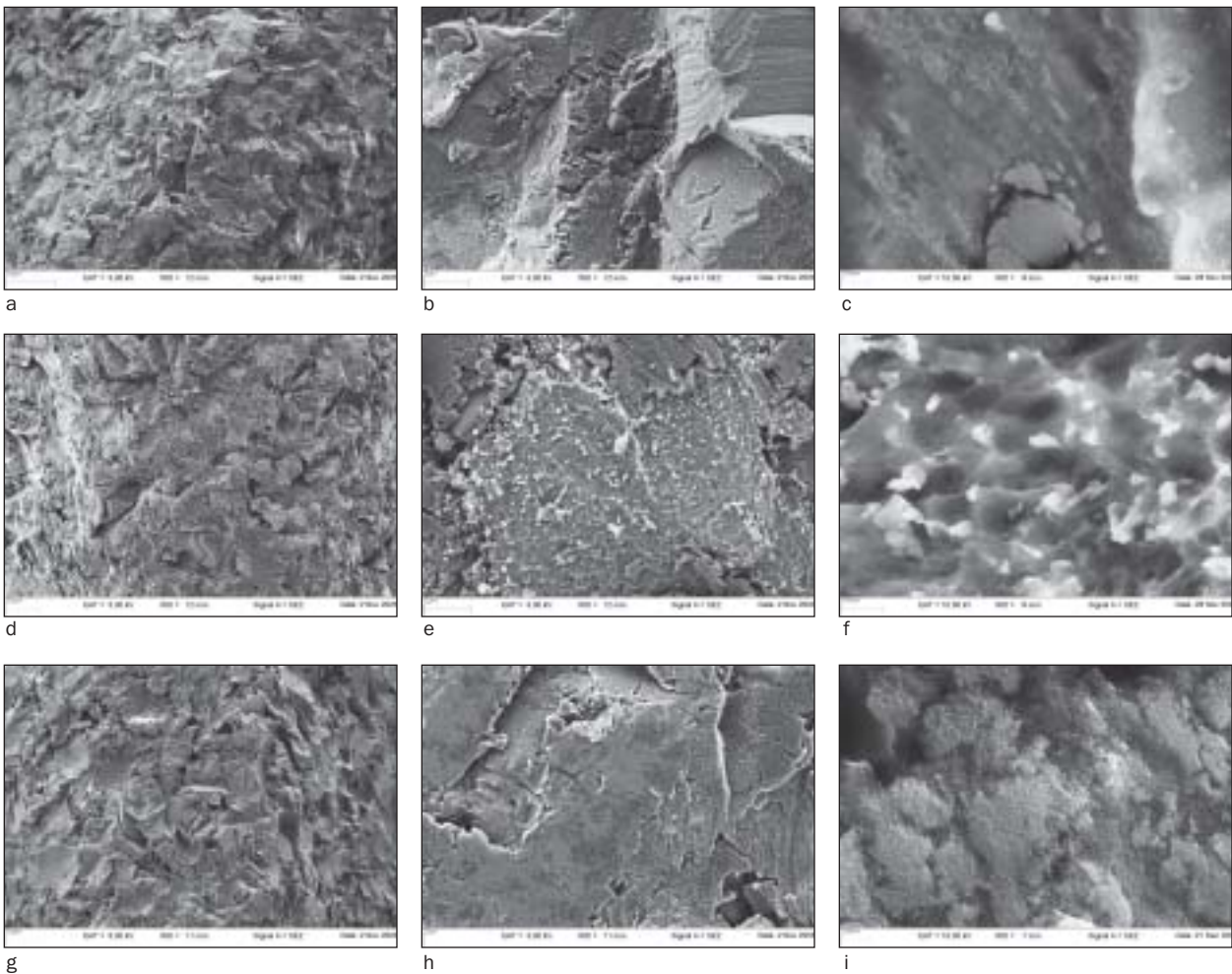

Fig 3 SEM micrographs of the blasted *(a, b, c)*, fluoride-treated *(d, e, f)* and nano-HA *(g, h, i)* implants at ×1,500 *(a, d, g)*, ×20,000 *(b, e, h)*, and ×125,000 magnification *(c, f, i)*.

Bone Response Evaluation

Removal Torque Tests. The results of the removal torque test after 4 weeks revealed a significant increase in retention for the F2 and nano-HA implants, whereas the F1 implant had a tendency toward higher values compared to the control implants. The mean values obtained for the control, F1, F2, and nano-HA implants were 29 ± 12 Ncm, 34 ± 11 Ncm, 36 ± 13 Ncm, and 37 ± 13 Ncm. No difference was observed between F1 and F2 implants showing that the experimental model selected was suitable.

Table 2	Removal Torque Values (Ncm)		
	Mean	**SD**	**Range**
Blasted	29	12	14–48
Blasted-F1	34	11	20–53
Blasted-F2	36	13	20–54
Blasted–nano-HA	37	13	17–54

(Statistical comparisons: Blasted vs Blasted-F1, $P < .1$; Blasted-F1 vs Blasted-F2, $P = .8$; $P = .04$; $P = .02$)

Histologic Analyses

Periosteal and endosteal callus formation was observed in all groups. The bone structure at the implant interface was immature, with a clearly distinguished line from the original cortical bone, as has been reported with similar healing period.[13,18] The bone-implant contact values calculated after a healing period of 4 weeks were 21.5% for the control group, 30.4% for the F1 group, 27.1% for the F2 group, and 35.8% for the nano-HA implant group, respectively. An interesting finding was the similar cortical bone formation among the groups. By contrast, in the endosteal area isolated bone formation was observed in contact with F1, F2, and nano-HA implants. For the control implants, no isolated bone formation from the original cortical bone was observed. The main goal of the histologic analyses was to perform a qualitative evaluation of the bone healing and development stage. However, a histomorphometric evaluation was also performed on 2 implant sections of each group. Thus, the analysis of bone-implant contact was based on a limited number of samples and should be interpreted with caution.

DISCUSSION

Potential benefits of the nano-HA crystals and fluoride nanostructures present at the implant surface may be divided in 2 parts based on the biomineralization theory. HA crystal precursors are initially found inside matrix vesicles, extracellular vesicles associated with mineralized forming tissue cells, such as osteoblasts and odontoblasts. Ca^{2+} and PO_4^{3-} accumulation inside these matrix vesicles will form noncrystalline amorphous calcium phosphates further transformed to HA (phase 1). Continuous growth of the crystals inside the matrix vesicles will expose the crystals to the extracellular fluid, after penetrating the matrix vesicle membranes (Phase 2).[19] The extravesicular HA crystals are deposited into the well-organized nanostructure of collagen molecules and act as nucleation sites for the continuous mineralization phenomenon. Adding extra ions to the interface, assuming some dissolution of the nano-HA may increase the HA formation inside the matrix vesicles (phase 1) and increase the continuous formation of the crystals located in the collagen fibrils network (phase 2). Furthermore, the nano-HA modified implants have structures of similar dimensions and similar chemical composition of the HA crystals found in bone. Thus, the surface of such implants may represent a binding site for molecules, such as collagen, after implant placement. Fluoride-treated implants have structures on the surface with similar dimensions as found in bone as well, but the potential chemical effect of fluoride ions follows a different route. The production of crystals in the matrix vesicles is controlled partially by alkaline phosphatase,[20] and fluoride has a direct stimulation effect on the alkaline phosphatase[21] related to increased osteoblast activity. Small amounts of fluoride greatly facilitated the kinetics of crystal formation,[22] and the fluoride-apatite formed is more stable than HA,[23] increasing the rate of fluoride-apatite precipitation, which may favorably affect the biomineralization of the bone. Recently, enhanced bone sialoprotein expression to fluoride-treated implants was related to increased bone-implant contact in rats after 3 weeks of healing.[24]

Surface chemical treatments can alter not only the chemical composition but also the surface topography. The topographical evaluation of the blasted and nano-HA implants evaluated by interferometer revealed microstructures with sharper edges and more pronounced differences of the peak and valley of the structures present at the surface compared to the fluoride-treated implants (Fig 2). This may explain the slight increase of the S_a value of the blasted and nano-HA implants compared to fluoride-treated implants. The slightly smooth surface of the fluoride-treated implants observed with interferometer corresponds well to the SEM images obtained at ×1,500 magnification (Fig 3). Finally, the developed surface

area ratio (S_{dr}) and density of summit (S_{ds}) parameters calculated on the interferometer were similar in all tested implants, and taking into account solely the slight difference in average height deviation (S_a), it is difficult to justify the differences observed between the removal torque values. Experiments with bone-forming cells in vitro demonstrated that osteoblast-like cell attachment,[25] proliferation, and differentiation[26] were affected by the surface microtopography. In vivo studies have demonstrated increased bone formation with moderately rough implants,[17,27] and clinical data have revealed enhanced bone formation in humans.[28,29] However, the surfaces evaluated in those studies had a clear difference in microtopography not observed in the present study, which could explain the different results observed. If the microroughness parameters alone are considered, the microtopography would be favored over the blasted implant, with the Sa value closer to the optimal value of 1.5 μm.[30] Therefore, the present results indicated that the roughness parameters at the micron level alone did not explain the differences in the removal torque values, where the results indicated higher bone anchorage of the F1 and nano-HA implants compared to blasted implants. Similar results have been reported[13] with fluoride-treated and blasted implants. Despite the slight decrease of S_a values, fluoride-treated implants exhibited an enhances bone formation compared to blasted implants placed in a rabbit model.

The only obvious topographical difference observed in the present study was at the nanometer scale, where the fluoride-treated and nano-HA implants had nanostructures situated over the microstructures, whereas the blasted implants failed to show these nanostructures (Fig 3). Bone response as evaluated by removal torque test revealed increased bone anchorage (F2 and nano-HA implants) or a tendency toward increased bone anchorage (F1) for the implants that exhibited such nanostructures compared to the control group. Some in vitro experiments have evaluated the effects of nanostructures and reported upregulation of bone sialoprotein,[31] increased osteoblast adhesion,[32] and proliferation,[33] probably mediated by specific proteins.[33] More recently, preosteoblast cells cultured on nano-HA modified surfaces revealed developed filopodia and lamellipodia.[34] These results may be related to increased bone healing after 4 weeks in rabbits found in the present study. Indeed, a previous in vivo study showed higher bone-implant contact to nano-HA modified implants compared to noncoated controls after a 4-week healing period, where the effect of the microstructures was removed by an electropolishing technique and the bone response was mainly dependent on the nano-HA structures.[12] Future experiments should address the potential effect of chemically modified implant nanotopography on bone response at longer healing periods. Surface modifications on the nano scale add knowledge to what is known about bone-implant interactions and represent an alternative to achieve better clinical results.

CONCLUSION

The chemical modifications used produced a nanotopography over the microstructures present at the blasted implants. Chemical analyses showed the presence of specific ions on the modified implants that together with the nanotopography observed may explain the differences in bone response.

ACKNOWLEDGMENTS

REFERENCES

1. Kasemo B. Biological surface science. Surface Sci 2002;500: 656–677.
2. Aumailley M, Gayraud B. Structure and biological activity of the extracellular matrix. J Mol Med 1998;76:253–265.
3. Adams JC. Cell-matrix contact structures. Cell Mol Life Sci 2001; 58:371–392.
4. Stevens MM, George JH. Exploring and engineering the cell surface interface. Science 2005;310:1135–1138.
5. Albrektsson T, Wennerberg A. Oral implant surfaces: Part 2— Review focusing on clinical knowledge of different surfaces. Int J Prosthodont 2004;17:544–564.
6. Curtis A, Wilkinson C. New depths in cell behaviour: Reactions of cells to nanotopography. Biochem Soc Symp 1999;65:15–26.
7. Friberg B, Jemt T, Lekholm U. Early failures in 4,641 consecutively placed Brånemark dental implants: A study from stage 1 surgery to the connection of completed prostheses. Int J Oral Maxillofac Implants 1991;6:142–146.
8. Jemt T, Lekholm U. Implant treatment in edentulous maxillae: A 5-year follow-up report on patients with different degrees of jaw resorption. Int J Oral Maxillofac Implants 1995;10:303–311.
9. Esposito M, Hirsch JM, Lekholm U, Thomsen P. Biological factors contributing to failures of osseointegrated oral implants. (I). Success criteria and epidemiology. Eur J Oral Sci 1998:527–551.
10. Johansson C, Albrektsson T. Integration of screw implants in the rabbit: A 1-year follow-up of removal torque of titanium implants. Int J Oral Maxillofac Implants 1987;2:69–75.
11. Meirelles L, Arvidsson A, Albrektsson T, Wennerberg A. Increased bone formation to unstable nano rough titanium implants. Clin Oral Implants Res 2007;18:326–332.
12. Meirelles L, Arvidsson A, Andersson M, Kjellin P, Albrektsson T, Wennerberg A. Nano hydroxyapatite structures influence early bone formation. J Biomed Mater Res A (in press).

13. Ellingsen JE, Johansson CB, Wennerberg A, Holmen A. Improved retention and bone-to-implant contact with fluoride-modified titanium implants. Int J Oral Maxillofac Implants 2004;19: 659–666.
14. Kjellin P, Andersson M. Synthetic nano-sized crystalline calcium phosphate and method of production. Sweden: SE-0401524-4, 2006:1–18.
15. Donath K, Breuner G. A method for the study of undecalcified bones and teeth with attached soft tissues. The Sage-Schliff (sawing and grinding) technique. J Oral Pathol 1982;11:318–326.
16. Johansson CB, Albrektsson T. A removal torque and histomorphometric study of commercially pure niobium and titanium implants in rabbit bone. Clin Oral Implants Res 1991;2:24–29.
17. Wennerberg A, Ektessabi A, Albrektsson T, Johansson C, Andersson B. A 1-year follow-up of implants of differing surface roughness placed in rabbit bone. Int J Oral Maxillofac Implants 1997;12:486–494.
18. Johansson CB, Han CH, Wennerberg A, Albrektsson T. A quantitative comparison of machined commercially pure titanium and titanium-aluminum-vanadium implants in rabbit bone. Int J Oral Maxillofac Implants 1998;13:315–321.
19. Anderson HC. Molecular biology of matrix vesicles. Clin Orthop Relat Res 1995:266–280.
20. Robison R. The possible significance of hexosephosphoric esters in ossification. Biochem J 1923;17:286–293.
21. Farley JR, Wergedal JE, Baylink DJ. Fluoride directly stimulates proliferation and alkaline phosphatase activity of bone-forming cells. Science 1983;222:330–332.
22. Eanes ED, Meyer JL. The influence of fluoride on apatite formation from unstable supersaturated solutions at pH 7.4. J Dent Res 1978;57:617–624.
23. Moreno EC, Kresak M, Zahradnik RT. Physicochemical aspects of fluoride-apatite systems relevant to the study of dental caries. Caries Res 1977;11(suppl 1):142–171.
24. Cooper LF, Zhou Y, Takebe J, et al. Fluoride modification effects on osteoblast behavior and bone formation at TiO$_2$ grit-blasted c.p. titanium endosseous implants. Biomaterials 2006;27: 926–936.
25. Bowers KT, Keller JC, Randolph BA, Wick DG, Michaels CM. Optimization of surface micromorphology for enhanced osteoblast responses in vitro. Int J Oral Maxillofac Implants 1992;7:302–310.
26. Martin JY, Schwartz Z, Hummert TW, et al. Effect of titanium surface roughness on proliferation, differentiation, and protein synthesis of human osteoblast-like cells (MG63). J Biomed Mater Res 1995;29:389–401.
27. Wennerberg A, Albrektsson T, Andersson B, Krol JJ. A histomorphometric and removal torque study of screw-shaped titanium implants with three different surface topographies. Clin Oral Implants Res 1995;6:24–30.
28. Ivanoff CJ, Widmark G, Johansson C, Wennerberg A. Histologic evaluation of bone response to oxidized and turned titanium micro-implants in human jawbone. Int J Oral Maxillofac Implants 2003;18:341–348.
29. Ivanoff CJ, Hallgren C, Widmark G, Sennerby L, Wennerberg A. Histologic evaluation of the bone integration of TiO(2) blasted and turned titanium microimplants in humans. Clin Oral Implants Res 2001;12:128–134.
30. Wennerberg A. On Surface Roughness and Implant Incorporation [PhD thesis]. Biomaterials/ Handicap Research. Göteborg, Sweden: Göteborg University, 1996.
31. de Oliveira PT, Nanci A. Nanotexturing of titanium-based surfaces upregulates expression of bone sialoprotein and osteopontin by cultured osteogenic cells. Biomaterials 2004;25:403–413.
32. Webster TJ, Siegel RW, Bizios R. Osteoblast adhesion on nanophase ceramics. Biomaterials 1999;20:1221–1227.
33. Webster TJ, Ergun C, Doremus RH, Siegel RW, Bizios R. Specific proteins mediate enhanced osteoblast adhesion on nanophase ceramics. J Biomed Mater Res 2000;51:475–483.
34. Zhu XL, Eibl O, Berthold C, Scheideler L, Geis-Gerstrofer J. Structural characterization of nanocrystalline hydroxyapatite and adhesion of pre-osteoblast cells. Nanotechnology 2006;17:2711–2721.